Available online at www.sciencedirect.com
SCIENCE DIRECT®
Journal of Magnetic Resonance 177 (2005) 228–235
JMR Journal of Magnetic Resonance
www.elsevier.com/locate/jmr

Initially linear echo-spacing dependence of $1/T_2$ measurements in many porous media with pore-scale inhomogeneous fields

Paola Fantazzini [a,*], Robert J.S. Brown [b]

[a] University of Bologna, Department of Physics, Viale Berti Pichat 6/2, 40127 Bologna, Italy
[b] 953 W. Bonita Ave., Claremont, CA 91711-4193, USA

Received 10 May 2005; revised 24 July 2005
Available online 8 September 2005

Abstract

For a liquid sample with unrestricted diffusion in a constant magnetic field gradient g, the increase R in $R_2 = 1/T_2$ for CPMG measurements is $\frac{1}{3}(\tau\gamma g)^2 D$, where γ is magnetogyric ratio, τ is half the echo spacing TE, and D is the diffusion constant. For measurements on samples of porous media with pore fluids and without externally applied gradients there may still be significant pore-scale local inhomogeneous fields due to susceptibility differences, whose contributions to R_2 depend on τ. Here, diffusion is not unrestricted nor is the field gradient constant. One class of approaches to this problem is to use an "effective gradient" or some kind of average gradient. Then, R_2 is often plotted against τ^2, with the effective gradient determined from the slope of some of the early points. In many cases, a replot of R_2 against τ instead of τ^2 shows a substantial straight-line interval, often including the earliest available points. In earlier work [G.C. Borgia, R.J.S. Brown, P. Fantazzini, Phys. Rev. E 51 (1995) 2104; R.J.S. Brown, P. Fantazzini, Phys. Rev. B 47 (1993) 14823] these features were noted, and attention was called to the fact that very large changes in field and gradient are likely for a small part of the pore fluid over distances very much smaller than pore dimensions. A truncated Cauchy–Lorentz (C–L) distribution of local fields in the pore space was used to explain observations, giving reduced effects of diffusion because of the averaging properties of the C–L distribution, the truncation being at approximately $\pm\frac{1}{2}\chi B_0$, where χ is the susceptibility difference. It was also noted that, when there is a narrow range of pore size a, over a range of about 40 of the parameter $\xi = \frac{1}{3}\chi v a^2/D$, where v is the frequency, R_2 does not depend much on pore size a nor on diffusion constant D. Examples are shown where plots of R_2 vs τ show better linear fits to the data for small τ values than do plots vs τ^2. The present work shows that, if both grain-scale and sample-scale gradients are present for samples with narrow ranges of T_2, it may be possible to identify the separate effects with the linear and quadratic coefficients in a second-order polynomial fit to the early data points. Of course, many porous media have wide pore size and T_2 distributions and hence wide ranges of ξ. For some of these wide distributions we have plotted R_2 vs τ for signal percentiles, normalized to total signal for shortest τ, again showing initially linear τ-dependence even when available data do not cover the longest and/or shortest T_2 values for all τ values. For the examples presented, both the intercepts and the initial slopes of the plots of R_2 vs τ increase systematically with signal percentile, starting at smallest R_2.

Keywords: Porous media; Susceptibility differences; Echo spacing; Diffusion; Field gradients

1. Introduction

For a CPMG measurement of T_2 for a liquid in bulk in a constant magnetic field gradient the measured increase R of $R_2 = 1/T_2$ is $\frac{1}{3}(\gamma g\tau)^2 D$, where g is the gradient, τ is half the echo spacing, and D is the diffusion coefficient. In this case, a plot of R_2 vs τ^2 has a slope $\frac{1}{3}\gamma^2 g^2 D$ and an intercept that gives R_0, the value of R_2 in the absence of gradient and diffusion effects. When the NMR signal is from a liquid confined in a porous medium, there are, however, two additional complica-

* Corresponding author. Fax: +39 051 209 0457.
E-mail address: paola.fantazzini@unibo.it (P. Fantazzini).

1090-7807/$ - see front matter © 2005 Elsevier Inc. All rights reserved.
doi:10.1016/j.jmr.2005.08.001

tions. One is that the diffusion of molecules of the fluid is restricted by the solid framework of the porous medium. The other is that there are usually significant grain-scale local inhomogeneous magnetic fields due to susceptibility differences between the solid and liquid. In some cases there may even be ferromagnetic mineral grains that produce significant local fields even in relatively weak B_0 fields. One class of approaches to local fields is by use of "effective gradients" [1]. However, the gradients of these local fields are definitely *not* everywhere the same, and, for a small fraction of the pore fluid, they can change substantially over distances much smaller than local pore dimensions.

Both of these complications interfere with the simple quadratic dependence of R on τ. Under frequently encountered circumstances the effects of diffusion over very short distances appear to lead to some loss of echo amplitude at very short times. In many cases the result appears to be a significant interval of approximately *linear*, rather than quadratic, increase of R_2 with τ, often including the points at the shortest available echo times. These effects were observed as far back as 1992 [2] and investigated further over the next several years [3–6]. However, this initially linear behavior and related features of the local fields from susceptibility differences have not been widely noted nor utilized where they might be relevant in work on fluids in porous media. For this reason, we gather in this paper some examples from widely varying sources and conditions to help illustrate the effects of local field changes over very short distances, and we also recall some features that have been described earlier.

In [3], it is shown that local field changes of the order of χB_0, where χ is the susceptibility difference between the solid matrix and the pore fluid and B_0 is the static NMR field, can occur with diffusion over distances very small compared with pore radius a and in times extremely short compared to a^2/D, thus disrupting the refocusing of echoes for parts of the pore fluid in times shorter than would be expected with quadratic τ-dependence. It is also shown that, although field singularities are possible in principle, the effective local fields are limited to approximately $\pm{}^1\!/_2\chi B_0$.

In [5], it is shown that the distribution of local fields in a porous medium has the Cauchy–Lorentz (C–L: Cauchy in statistics and Lorentz in Physics, $1/[1+x^2]$) form, truncated or tapered to zero at roughly $\pm{}^1\!/_2\chi B_0$. The complete C–L distribution of phases corresponds to simple exponential decay. An important property of the C–L distribution is that averaging (for instance, by diffusion) of many samples does *not* narrow the distribution, as it does for the more familiar Gaussian distribution. There is a tendency for simple-exponential FIDs (free induction decay), and examples are shown [5,6] of Hahn echo decay reaching the asymptotic slope of the FID on log plots, approximately ${}^1\!/_3\chi v$, where v is the NMR frequency. This FID decay rate is, in turn the asymptotic rate for CPMG data as a function of τ. The slope of the linear portion of R_2 vs τ for CPMG data is proportional to $(\chi v)^2$, whereas the asymptote (FID rate) is proportional to χv. The truncation of the C–L distribution puts some limits on these properties. A complete C–L distribution results from randomly placed point dipoles [7], and strictly exponential FID decay, independent of diffusion coefficient D, has been observed.

Sen and Axelrod [8] have computed local fields and displayed a distribution which they describe as "a Lorentzian which has been clipped at the wing." Audoly et al. [9] have shown that the internal field changes rapidly with position in some locations at edges of pores and that the magnetic field correlation function is intimately related to the structure factor of the porous medium. Chen et al. [10] have shown that distributions of components of the gradient, as well as the field, have the C–L form. They also note that the magnetic susceptibility of many porous rocks is high enough that the susceptibility difference χ does not depend much on the pore fluid, so that the internal fields are about the same for a partially saturated rock as for a fully saturated one. They found single-exponential FID decay ($T_{2\text{-FID}} = 127$ μs) for decay by a factor of 100 for water in Berea sandstone, notwithstanding the multiexponential T_1 and $T_{2\text{-CPMG}}$ decay; presumably, the C–L field distributions, which affect the FID, do not directly depend on pore size in porous media with wide distributions of pore sizes.

In [5], for samples with narrow ranges of pore sizes and relaxation times, CPMG data were taken over ranges of pore size a, diffusion constant D, and measurement frequency v. The product of the frequency difference ${}^1\!/_3\chi v$ and the diffusion time a^2/D gives a dimensionless regime parameter $\xi = {}^1\!/_3\chi v a^2/D$, not involving the echo time. For a range of ξ over a factor of about 40, R had very little dependence on a or D.

With very slow diffusion, the missing tails of the truncated C–L distributions of fields can lead to a very short time [5,6] of initially quadratic R_2 vs τ dependence, which is for many data sets shorter than the time of the first available data point. A linear extrapolation of R_2 vs τ data to $\tau = 0$ may give an underestimate of the intercept $R_0 = 1/T_2(\tau \to 0)$, the value corrected for inhomogeneous field effects. In these cases, however, a quadratic fit to early points gives an overestimate, often a higher value than that of the first data point. At the other extreme, with very fast diffusion, the missing tails allow line narrowing.

Whether R_2 increases linearly or quadratically at short times, the increase saturates for fluids in porous media at longer echo spacings. In [5], it was found that the saturation of the initially linear curves for narrow distributions were well fit by a simple arctangent

function of the form $R_2 \approx r_0 + b\tau_0 \tan^{-1}(\tau/\tau_0)$, where r_0 is an estimate of R_0, the slope is b for $\tau \ll \tau_0$, and τ_0 is a saturation time for the τ dependence. We have encountered numerous data sets well fit by this form. We have also noted published data plotted in other forms than R_2 vs τ, where scanning and replotting R_2 against τ shows the initially linear arctangent form, and several examples will be given.

In many cases non-local gradients of instrumental origin, either pulsed or steady, are applied, and in some NMR instruments geometrical factors may make large field gradients unavoidable. We show here that a fit to the R_2 data at short times by a second-order polynomial may offer a means of separating the effects of local and non-local inhomogeneous fields when the two effects are comparable.

Finally, we introduce plots of the R_2 values of various signal percentiles for CPMG T_2 distributions for samples with wide distributions of T_2 as a means of demonstrating the initially linear τ-dependence for wide distributions, even when the data cannot cover the longest and/or shortest T_2 values.

2. Narrow distributions of pore sizes and relaxation times

For samples with narrow distributions of transverse relaxation rates R_2 the various representative rates, such as mean rate, reciprocal mean time, geometric mean rate, or rate at peak, are not drastically different and should vary with τ in approximately the same manner, whether linear or quadratic.

Fig. 1 shows recent CPMG measurements by Fantazzini et al. [11] of R_2 vs τ at 20 MHz for a water-saturated ceramic material with a narrow distribution of pore sizes. The T_2 values used were those at the peaks, which were fairly symmetrical on logarithmic displays except for very small tails toward short times. Gaussian halfwidths were in the 0.3–0.4 Np range. Thus, the T_2 values at the peaks approximate geometric-mean (log-mean) times, excluding the small tails. The $1/T_2$ data are well approximated by the arctangent curve shown, and the first several points are in the nearly linear part of the curve. The intercept r_0 corresponds to $T_2 =$ 88 ms, and T_1 is 231 ms, about 2.6 times greater. Since this is a reasonable T_1/T_2 ratio for water in porous media, it is probable that R_0 was not greatly underestimated by the extrapolation.

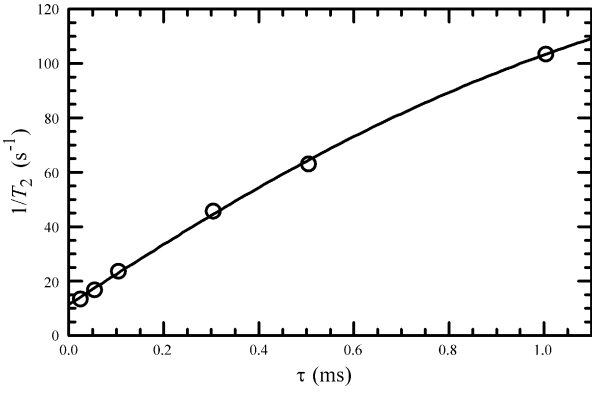

Fig. 1. $1/T_2 = R_2$ vs τ at 20 MHz for a water-saturated ceramic material with a narrow distribution of pore sizes. The solid curve is the arctangent fit, of the form $r_0 + b\tau_0 \tan^{-1}(\tau/\tau_0)$.

Fig. 2 shows recent measurements by Casieri et al. [12] and Fantazzini [13] at 20 MHz on two samples of the same porous porcelain, one a small sample in the uniform field of a conventional laboratory NMR instrument (lower curve), and the other a larger sample placed next to a one-sided NMR instrument [14] used for measurements on surfaces of large objects, such as statues, paintings, or buildings (upper curve). In both cases geometric-mean (log mean) T_2 values were used. The one-sided NMR produces an unavoidable non-local gradient in addition to the grain-scale local gradients due to susceptibility differences. For small phase shifts, signal decay is determined by mean-square phase [3], and the randomly directed local fields do not give cross terms with the non-local fields of the instrument, suggesting that the echo decay due to the local and non-local fields may be nearly independent at short times. The lower curve is fit by the arctangent function. The upper curve, fit to the data from the one-sided NMR, is of the form $r_0 + b\tau + c\tau^2$, fit to the data only up to τ values for which the lower curve is approximately linear. The intercepts r_0 and initial slopes b for the two fits are nearly identical and are represented by the straight line. It would appear that the linear term for the upper curve represents the effects of the local fields due to susceptibility differences and that the τ^2 term represents the effects

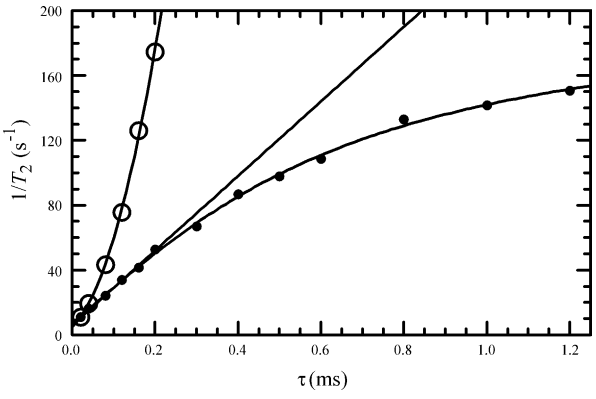

Fig. 2. Water-saturated porous porcelain samples. Lower points are for measurements in the uniform field of a laboratory NMR instrument, fit by the arctangent function $r_0 + b\tau_0 \tan^{-1}(\tau/\tau_0)$. Upper points are by a one-sided NMR instrument that produces a substantial gradient, with the early points fit by the form $r_0 + b\tau + c\tau^2$. The values of intercept r_0 and initial slope b from the two measurements are essentially the same and represented by the straight line.

of the large-scale field of the instrument. The upper data are *not* fit well by the form $r_0 + c\tau^2$, without the linear term.

Fig. 3 was obtained by scanning Fig. 3 of a 1990 paper by Rozenman et al. [15] and replotting their parameter $R(\tau)$–$R(0.2)$ against τ instead of τ^2, giving a good arctangent fit. The T_2 values were single-exponential fits to the decay data and taken for three temperatures, for which the $1/T_2$ values were averaged for Fig. 3. The sample was liver excised from a rat that had been treated with a contrast agent containing superparamagnetic iron oxide (SPIO). The CPMG measurements were at 360 MHz. The control sample, without SPIO, did not follow this pattern.

Fig. 4 was obtained by scanning Fig. 2 of a 1990 paper by Kleinberg and Horsfield [16] and making a linear plot instead of the log–log plot. The T_2 values were from fits to the decay data by the two-adjustable-parameter stretched-exponential form, $\exp[-(2n\tau/T_2)^{\alpha}]$, where n is the echo number. The data are for a porous limestone rock sample saturated with brine. This sample may have had substantial ranges of T_2 values, represented by the parameter α, but α was not given. The authors presumably took CPMG data that adequately covered the ranges of T_2 at all τ values, giving a single relaxation time parameter as a function of τ, leading this sample to be included under "narrow distributions." Measurements were made at 5, 40, and 90 MHz. At each frequency the data are well fit by the arctangent, although the effect is small at the lowest frequency and saturates quickly at the highest.

Most of the points of Fig. 5 were obtained by scanning Fig. 15 of a recent paper by Zhang etal. [17] and plotting $1/T_2$ against τ. The data are for CPMG measurements at 2 MHz on slurries of the iron-containing mineral chlorite with brine, hexane, and crude oil, and T_2 values are at peaks. The curve for Soltrol-130 was not replotted, because the early points could not be read from the scanned figure. As was appropriate to the authors' purpose of verifying computed average or effective gradients, the $\tau = 0.1$ ms points for water and hexane were omitted from the published figure, and R_2 was plotted against τ^2. For the present Fig. 5 the $\tau = 0.1$ ms point for hexane was obtained from the distribution shown in Fig. 14 of [17]. The T_2 distributions for $\tau = 0.1$ ms for all the fluids in chlorite slurries are given in Fig. 8 of [18], and the values for brine and crude oil are taken from the peaks of these distributions. The points for $\tau = 0.1$ are far below the straight lines drawn in the plots against τ^2, and the rates extrapolated to $\tau^2 = 0$ are well above the measured rates for $\tau = 0.1$ ms.

The points in the plots of R_2 against τ in Fig. 5 lie close to the straight lines shown. However, the straight lines for brine and hexane extrapolate to rates lower than $R_0 > 1/T_1$, which is 10.5 s^{-1} for the brine slurry and 1.05 s^{-1} for the hexane slurry; using the authors' tentative value 1.6 for R_0T_1 suggests that the R_0 should be about 17 s^{-1} for the brine slurry and 1.7 for the

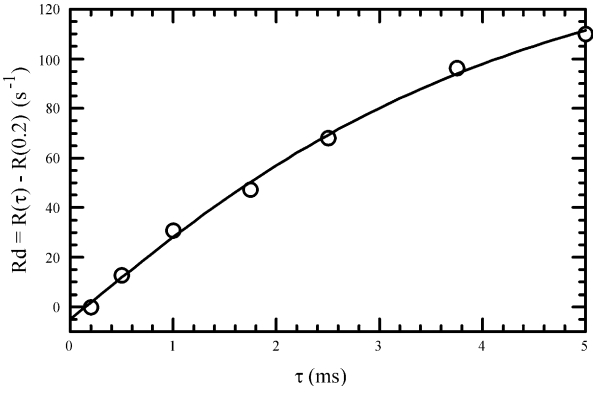

Fig. 3. CPMG measurements, from a paper by Rozenman, Zou, and Kantor, at 360 MHz for liver excised from a rat that had been treated with a contrast agent containing superparamagnetic iron oxide (SPIO). The solid line is the arctangent fit.

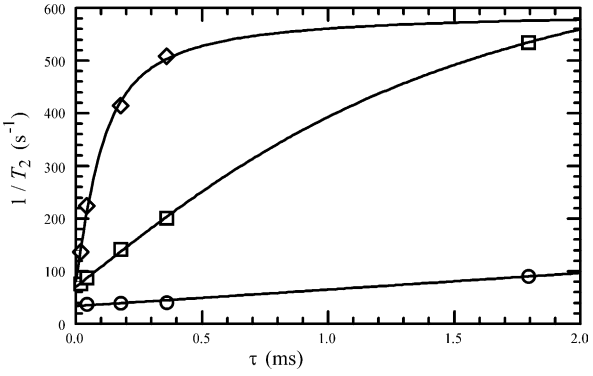

Fig. 4. Measurements, from a paper by Kleinberg and Horsfield, on a porous limestone rock sample saturated with brine, with CPMG measurements at 5, 40, and 90 MHz. The solid curves are the arctangent fits.

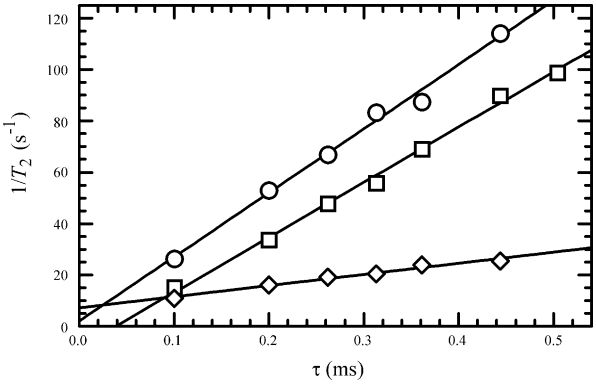

Fig. 5. CPMG measurements at 2 MHz on slurries of the iron-containing mineral chlorite with brine (top), hexane (middle), and crude oil (bottom). The lines for brine and hexane extrapolate to rates lower than those in the absence of the inhomogeneous field and diffusion effects, $R_0 > 1/T_1$, and they cross the estimated R_0 values of brine and hexane at about 60 and 45 μs, respectively. See text.

hexane. The line for brine crosses 17 at about $\tau = 60$ μs, and the line for hexane crosses 1.7 at about 45 μs. If the points are correct as measured and as scanned and replotted, there may be for this system a time of the order of 45–60 μs, shorter than the first available measurement time, before the linear increase of R with τ begins.

3. Wide distributions

For samples with wide distributions of pore sizes and relaxation times one may represent the relaxation behavior of a sample by a single time, such as geometric-mean time. However, it may not be clear what useful physical interpretation is to be made of the τ-dependence of such a parameter, and there are often serious problems in defining a meaningful R_2 from available measurements.

If the shortest T_2 at the longest τ is not significantly longer than the longest τ, then some of the magnetization represented at the shorter τ's is not included in the distributions for the longer τ's. If the shortest τ is not sufficiently short, even that distribution may not include all the magnetization.

At the shorter τ values, the maximum number of echoes available (8000 for the two examples below) may not be enough to cover adequately the longest T_2's. In most cases an adequate phase-cycling sequence is used to give zero baseline at sufficiently long times. Therefore, magnetization is not lost at long times, but relaxation times are not determined at long times if there are not enough echoes. For instance, if $\tau = 20$ μs and there are 8000 echoes, the last echo is at 320 ms, which is shorter than the longest T_2 components found in many porous media.

If at a given τ we do not have adequate data coverage at short and/or long times, we may still have intermediate ranges of R_2's adequately covered by data to give distributions good enough to give some τ-dependence information. Fortunately, even if small R_2's (long times) are not adequately covered, we can have the correct *cumulative* distributions of signal vs R_2, starting at small R_2, for intermediate ranges. We can now track the τ-dependence of the R_2 values corresponding to some fixed cumulative signal, assuming that instrumental gains and other parameters are held fixed for data with different τ's. It is probably convenient to normalize these cumulative signals to the total signal at the shortest τ or else to the total signal extrapolated to $\tau \to 0$. We can then follow the τ-dependence of various signal percentiles, even if we do not have adequate data coverage for the lowest and/or highest percentiles.

3.1. First example: water-saturated brick material

Fig. 6 shows CPMG T_2 distributions computed with UPEN [19] for a sample of iron-containing brick material saturated with water. Fig. 7 shows percentile vs R_2 for the data from Fig. 6, and Fig. 8 shows the τ-dependence of R_2 at five-percentile intervals from 15 to 40%. In Figs. 6 and 7 it can be seen that about 10% of the signal has much lower R_2 (longer T_2) than the rest and that the data are not good enough to give good distributions much below the 15th percentile for this small amount of signal. At the other end, at percentiles 50 and higher, the relaxation at short times is not adequately covered by data with the longest τ. Awkwardly, the relaxation times become shorter with increasing τ, while the times of the first data points become longer. In any case, it is clear that τ-dependence is approximately linear, not quadratic, from $\tau = 0.02$ to 0.1 ms for the 15–40 percentiles.

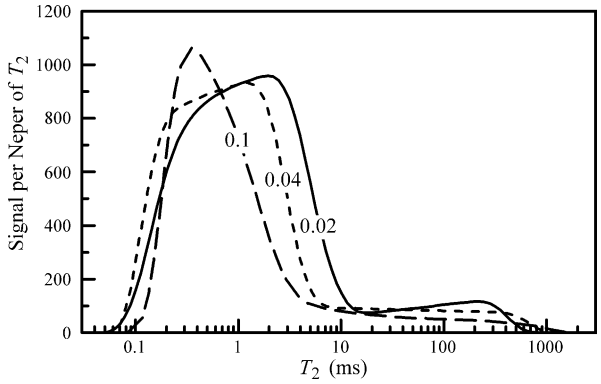

Fig. 6. CPMG T_2 distributions for an iron-containing brick material saturated with water. The curves are labeled with τ in ms. About 10% of the signal is at much longer T_2 than the rest and cannot be determined with sufficient accuracy for the percentile plots.

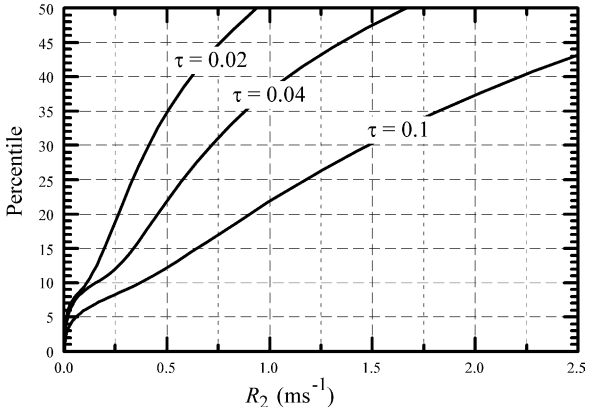

Fig. 7. Signal percentiles from the data for Fig. 6, relative to total signal extrapolated to $\tau \to 0$, as functions of $R_2 = 1/T_2$ for $\tau = 0.02$, 0.04, and 0.1 ms.

3.2. Second example

Fig. 9 shows T_2 distributions for a water-saturated sandstone rock sample, computed with UPEN [19], for

five values of the half-echo-spacing τ from 15 to 100 μs. For $\tau = 15$ μs, the signal-to-noise ratio is 81, and substantial amplitudes extend from about 0.07 to 350 ms, a ratio of 5000. With data points from 30 μs it is clear that any signal with T_2 below 70 μs must have T_2 well below 30 μs.

The relative values of total signal for the curves of Fig. 9 are, in order of increasing τ, 1.00, 0.89, 0.82, 0.77, and 0.77. Increase of τ from 15 to 30 μs shifts 11% of the total signal to T_2 values well below 60 μs, with the observable distribution at baseline below 150 μs. This is presumably a diffusion or exchange effect that defeats refocusing for some of the signal represented by the shelf extending from 70 to 350 μs in the 15 μs curve. More signal is lost in the next two τ steps but not in the last step. Otherwise, we see the familiar transfer of signal to shorter T_2 values, for instance from the 10 to 40 ms peaks to the range from 1 to 5 ms.

Fig. 10 shows cumulative distributions for the data of Fig. 9, normalized to the total signal for the shortest τ. The horizontal lines are at 10-percentile intervals. The file for Fig. 10 can be used with many combinations of linear scales to read T_2 for combinations of percentile and τ, then using $R_2 = 1000/T_2$ to make tables with R_2 in s^{-1}.

Fig. 11 shows R_2 vs τ at 10-percentile intervals up to 80%. As seen in Fig. 10, only the first three curves (shortest τ values) reach 80%, and only the first passes 90%, going to 100% by definition. Fits to the 10–40% curves are arctangent functions; fit to the 50% curve is linear; fits to the 60–80% curves are second-order polynomials. The fits to the 60–80% curves require the linear

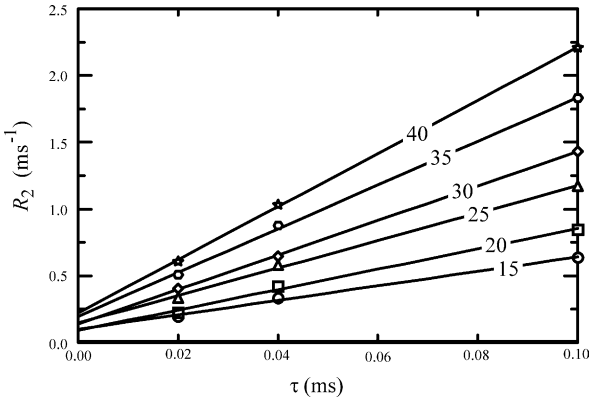

Fig. 8. Plots of R_2 vs τ from Fig. 7 at 5% intervals from 15 to 40%. The straight lines are best fits to the sets of three points.

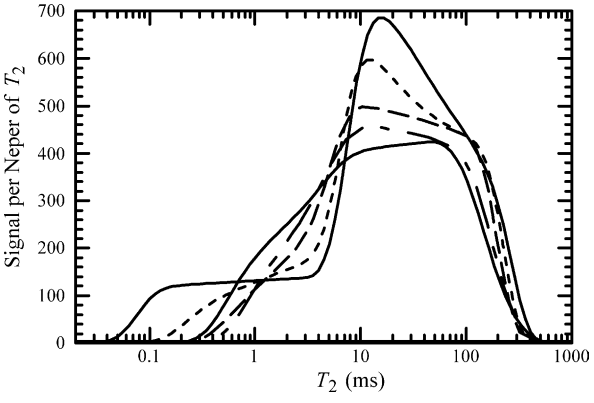

Fig. 9. T_2 distributions for five values of $\tau = TE/2$. From top to bottom at 20 ms, τ values are 15, 30, 45, 75, and 100 μs.

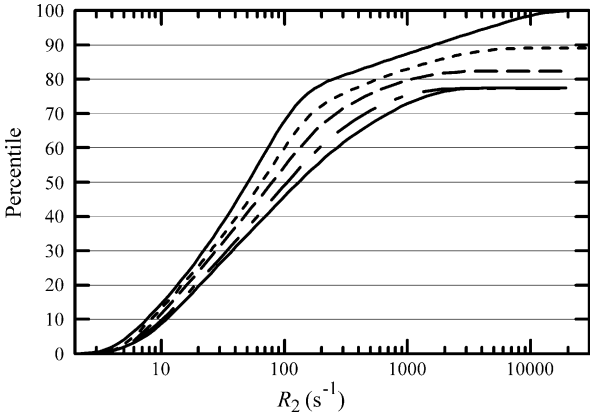

Fig. 10. Percentile levels for combinations of R_2 and τ. Left-to-right, τ values are 15, 30, 45, 75, and 100 μs. Percentile levels represent cumulative signal relative to total signal for $\tau = 15$ μs.

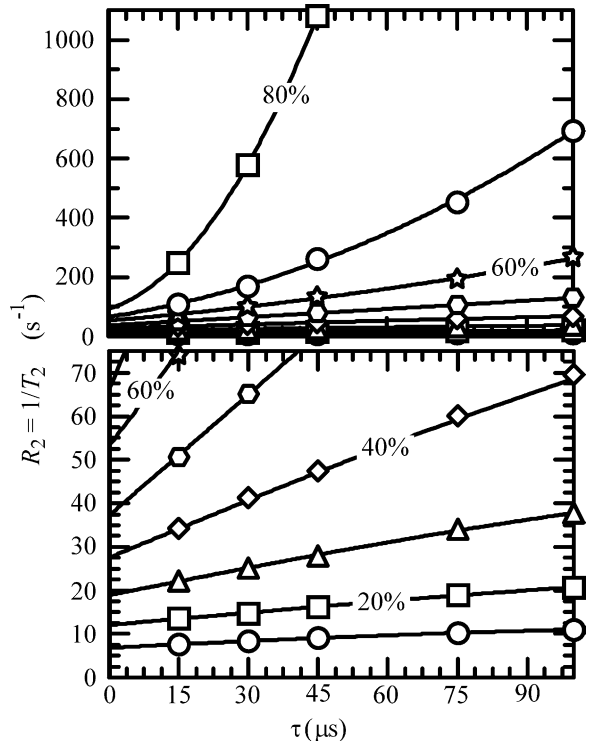

Fig. 11. R_2 vs τ at 10-percentile intervals for percentiles from 10 to 80, increasing upward. The solid lines are arctangent fits for 10–40%, straight line for 50%, and second-order polynomials for 60–80%. All three forms of fit include intercept and slope as fit parameters.

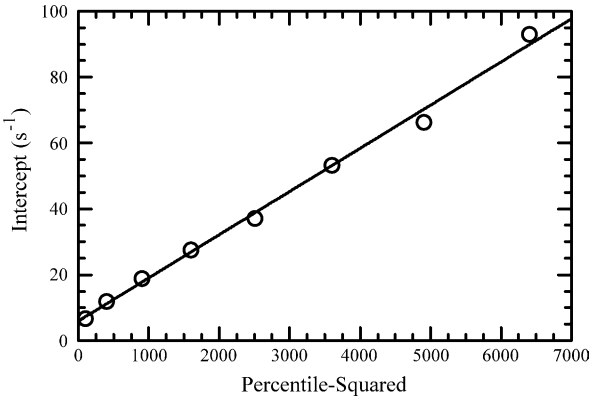

Fig. 12. The intercepts of the fitted curves in Fig. 11 plotted against percentile-squared.

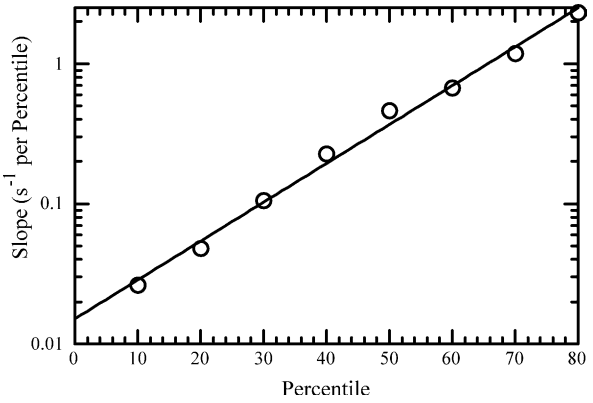

Fig. 13. The slopes of the fitted curves in Fig. 11 on semi-log plots against percentile.

term; the data are not adequately fit by the intercept and quadratic terms only.

It can be seen in Fig. 11 that the intercepts and slopes both increase systematically with percentile. Fig. 12 shows that intercept increases roughly as percentile-squared, and Fig. 13 shows that slope increases roughly exponentially with percentile. At this time we do not have reason to expect any particular forms for dependence of intercept or slope on percentile or even to expect monotonic variation for porous media in general.

4. Conclusions

Many porous media have sufficiently uniform pore structures that distributions of T_2 from CPMG measurements are narrow enough to give reasonably well-defined values of $1/T_2$ and their dependence on the half-echo-spacing τ. There is a wide variety of these fluid-saturated porous media for which CPMG measurements of $1/T_2$ show substantial early intervals of approximately linear τ-dependence when there are grain-scale local inhomogeneous fields due to susceptibility differences. This is in contrast to the τ^2-dependence for bulk fluid in a fixed gradient or even the initial τ^2-dependence for a fluid in a porous medium to which a strong non-local gradient is applied, either intentionally or because of the geometry of the instrument.

In some cases of samples with narrow distributions of relaxation times where the effects of local and non-local gradients are comparable, it may be possible to separate the two effects by the linear and quadratic coefficients in a second-order polynomial fit to the early part of the data.

Also some porous media with wide T_2 distributions show initially linear dependence of $1/T_2$ on τ. This has been shown even for samples where, for some or all τ values, the relaxation is not covered adequately at long and/or short times. To demonstrate this, R_2 vs τ has been plotted at various percentiles of signal relative to the total signal at the shortest τ, that is, the R_2 values for which fixed absolute amounts of signal have longer relaxation times. In the two examples shown, the initial slopes of R_2 vs τ are significant at all percentile levels.

The interpretation of the percentile data may not be simple for a complex porous material. For instance, one cannot be sure that a given small percentile range necessarily represents an identifiable subset of the nuclei or that the same nuclei are represented for different τ values. One might assume that the intercept values of $1/T_2$ vs τ are due to surface relaxation without inhomogeneous-field effects, giving the usual interpretation in terms of pore sizes, with the usual limitations in addition to the additional uncertainty of interpretation of the percentile data.

In any case, the effects of local inhomogeneous fields from susceptibility differences in many porous media saturated with fluids appear to lead to initially linear dependence on the echo-spacing for CPMG measurements of $1/T_2$.

Acknowledgments

The authors thank C. Garavaglia, F. Peddis, B. Ravaglia, and C. Vescogni for technical assistance. This work was supported by University of Bologna (Funds for selected research topics) and MIUR (FIRB 2001).

References

[1] M.D. Hürlimann, Effective gradients in porous media due to susceptibility differences, J. Magn. Reson. 131 (1998) 232–240.
[2] G.C. Borgia, R.J.S. Brown, P. Fantazzini, E. Mesini, G. Valdrè, Diffusion-weighted spatial information from ^{1}H relaxation in restricted geometries, Il Nuovo Cimento D 14 (1992) 745–759.
[3] R.J.S. Brown, P. Fantazzini, Conditions for initial quasilinear T_2^{-1} for Carr–Purcell–Meiboom–Gill NMR with diffusion and susceptibility differences in porous media and tissues, Phys. Rev. B 47 (1993) 14823–14834.

[4] R.J.S. Brown, P. Fantazzini, Taking, processing, and interpreting spin-echo data in porous media and tissues, Magn. Reson. Imaging 12 (1994) 175–178.
[5] G.C. Borgia, R.J.S. Brown, P. Fantazzini, Scaling of spin-echo amplitudes with frequency, diffusion coefficient, pore-size, and susceptibility difference for the NMR of fluids in porous media and biological tissues, Phys. Rev. E 51 (1995) 2104–2114.
[6] G.C. Borgia, R.J.S. Brown, P. Fantazzini, The effect of diffusion and susceptibility differences on T_2 measurements for fluids in porous media and biological tissues, Magn. Reson. Imaging 14 (1996) 731–736.
[7] R.J.S. Brown, Distribution of fields from randomly placed dipoles: free-precession signal decay as result of magnetic grains, Phys. Rev. 121 (1961) 1379–1382.
[8] P.N. Sen, S. Axelrod, Inhomogeneity in local magnetic field due to susceptibility contrast, J. Appl. Phys. 86 (1999) 4548–4554.
[9] B. Audoly, P.N. Sen, S. Ryu, Y.-Q. Song, Correlation functions for homogeneous magnetic field in random media with application to a dense random pack of spheres, J. Magn. Reson. 164 (2003) 154–159.
[10] Q. Chen, A.E. Marble, B.G. Colpitts, B.J. Balcom, The internal magnetic field distribution, and single exponential magnetic resonance free induction decay, in rocks, J. Magn. Reson. 175 (2005) 300–308.
[11] P. Fantazzini, A. Salem, G. Timellini, A. Tucci, R. Viola, Microstructure changes in fired ceramics quantified by magnetic resonance relaxation and imaging, J. Appl. Phys. 94 (2003) 5337–5342.
[12] C. Casieri, F. De Luca, P. Fantazzini, Pore size evaluation by single-sided nuclear magnetic resonance measurements: compensation of water self-diffusion effect on transverse relaxation, J. Appl. Phys. 97 (2005) 043901 (1–10).
[13] P. Fantazzini, Magnetic resonance for fluids in porous media at the University of Bologna, Magn. Reson. Imaging 23 (2005) 125–131.
[14] G. Eidman, R. Savelsberg, P. Blümler, B. Blümich, The NMR MOUSE, a mobile universal surface explorer, J. Magn. Reson. 122 (1996) 104–109.
[15] Y. Rozenman, X. Zou, H.L. Kantor, Signal losses induced by superparamagnetic iron oxide particles in NMR spin-echo images: the role of diffusion, Magn. Reson. Med. 14 (1990) 31–39.
[16] R.L. Kleinberg, M.A. Horsfield, Transverse relaxation processes in porous sedimentary rock, J. Magn. Reson. 88 (1990) 9–19.
[17] G.Q. Zhang, G.J. Hirasaki, W.V. House, Internal field gradients in porous media, Petrophysics 44 (2003) 422–434.
[18] G.Q. Zhang, G.J. Hirasaki, W.V. House, Effect of internal field gradients on NMR measurements, Petrophysics 42 (2001) 37–47.
[19] G.C. Borgia, R.J.S. Brown, P. Fantazzini, Uniform-penalty inversion of multiexponential decay data II. Data spacing, T_2 data, systematic data errors, and diagnostics, J. Magn. Reson. 147 (2000) 273–285.